Compound semiconductor oxide antireflection coatings

K. J. Knopp, R. P. Mirin, K. A. Bertness, K. L. Silverman,[a] and D. H. Christensen
National Institute of Standards and Technology, 325 Broadway MS 815.04, Boulder, Colorado 80303

(Received 12 August 1999; accepted for publication 20 January 2000)

We report the development of high quality, broad-bandwidth, antireflection (AR) coatings using the low index provided by wet thermally oxidized $Al_{0.98}Ga_{0.02}As$. We address the design criteria, fabrication, and characterizations of AR coatings composed of surface and buried oxide layers on GaAs. We show, using native-oxide dispersion data, that surface oxide coatings can be designed to offer a nearly zero minimum of reflectance and a reflectance of <1% over bandwidths as large as 500 nm. Surface coatings having a reflectance minimum of 0.4% and a reflectance of <1% over >250 nm have been experimentally demonstrated at a design wavelength of 1 micrometer. Additionally, buried oxide coatings can be designed with an $Al_xGa_{1-x}As$ matching layer of any composition to exactly match the admittance of any substrate with effective index between 2.5 and 3.5. We have demonstrated buried oxide coatings, also designed for 1 micrometer, having a reflectance minimum of 0.4% and a reflectance of <1% over 21 nm. The calculated optical scattering loss from measured roughness data indicates that reflectance minima as low as 10^{-4}% are ultimately achievable with native-oxide antireflection coatings. [S0021-8979(00)01709-6]

I. INTRODUCTION

The wet thermal oxidation of aluminum rich III–V compound semiconductors creates a dense and stable "native-oxide" film with tremendous versatility.[1] This electrically insulating and low refractive index oxide material has been used for current and optical-mode confinement in both edge-emitting[2] and vertical-cavity surface-emitting lasers (VCSELs).[3] Native oxides have also been used in the formation of low-loss and broad-bandwidth Al_xO_y-GaAs distributed Bragg reflectors (DBRs) for VCSELs, spatial light modulators, solar cells, and light-emitting diodes.[4] Many of these optoelectronic devices and others, such as photodetectors and saturable Bragg reflectors, benefit from broad-bandwidth antireflection (AR) coatings.

Traditionally, device designs in need of passivation layers, insulating layers, broad-bandwidth DBRs and AR coatings have used evaporated or sputtered dielectrics (for example, silicon dioxide, silicon nitride, and aluminum oxide). Native-oxide technology is now allowing innovative and higher performance all-epitaxially grown optoelectronic devices to be fabricated without the need for any additional deposition techniques beyond the semiconductor epitaxy.

In this article, we report the development of high quality (<0.5% reflectance), broad-bandwidth (<1% over 250 nm), antireflection coatings using the low index provided by native-oxide films. These native-oxide AR coatings reduce manufacturing complexities and promote integration with other native-oxide technologies. Furthermore, since these coatings are simple to manufacture and can be selectively etched from GaAs, they are suitable as *in situ* AR coatings for optical microlithography.[5] Throughout this article, we address the design criteria, fabrication, and characterizations of AR coatings composed of surface and buried oxide layers on GaAs. We consider manufacturing and device integration issues and demonstrate their application to the multilayer structure of a saturable absorber mirror.

[a]Electronic mail: silverma@boulder.nist.gov

II. THEORY

A. Single layer antireflection coating

The simplest AR coating uses a single film on top of a substrate to match the admittance of the incident medium to that of the substrate. The condition for proper matching of the substrate is well known.[6] To achieve zero reflectance at one wavelength with this coating, the sum of the two wave vectors reflected from the medium interfaces must be 0. This is accomplished if they are 180° out of phase (quarter wavelength layers) and if the two reflection coefficients are equal. Setting the reflection coefficients equal sets the relationship between the optical index of the substrate (n_2), film (n_1), and incident medium (n_0),

$$n_1^2 = n_0 n_2. \tag{1}$$

Using an incident medium of air and an index of refraction of 3.46 for GaAs at a wavelength of 1 μm, the calculated index for the matching film is 1.86. The index of wet-oxidized $Al_xGa_{1-x}As$ is ~1.57 while electron-beam-deposited Al_2O_3 has a higher index, near 1.77.[7] Unless the index of the oxide exactly matches the square root of the substrate index, there will not be a point of zero reflectance, but rather a point of minimum reflectance. For a matching layer index of 1.57, the calculated minimum reflectance is 2.8%. For electron beam deposited Al_2O_3, the calculated minimum reflectance is 0.25%. Figure 1 shows the effect of the matching-layer index on the minimum reflectance. Figure 2 illustrates the reflectance from a one-layer quarter-wave coating on a GaAs substrate with $n_1 = 1.57$ (for all wavelengths). The reflectance of uncoated GaAs is also shown for comparison. The reflectance is substantially reduced over the entire region. The coating exhibits less than 5% reflectance over a 295 nm range centered around the design wavelength

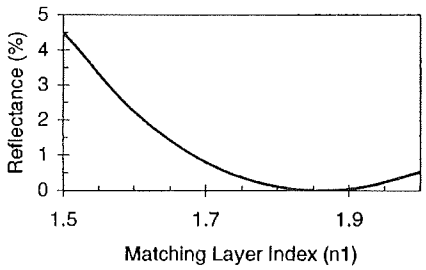

FIG. 1. Plot illustrating the minimum reflectance achievable for a given matching-layer index of a single-layer AR coating on GaAs at a wavelength of 1 μm.

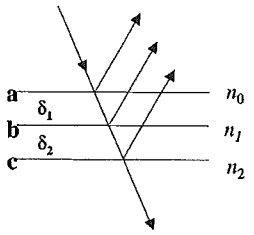

FIG. 3. The vector diagram for a two layer coating where n_0, n_1, n_2, and n_3 are the indices of refraction of the incident medium, first matching film layer, second film layer, and substrate, respectively. δ_1 and δ_2 are the phase thicknesses of the film layers. The three material interfaces are labeled *a*, *b*, and *c*.

of 1 μm. To broaden the region of low reflectance and further reduce the reflectance below that of a matching layer of wet-oxidized $Al_xGa_{1-x}As$ on GaAs, more layers must be added to the design.

B. Two layer antireflection coating (quarter–quarter)

The disadvantage of the single-layer coating is the limited number of adjustable parameters (i.e., the matching layer index and thickness are fixed). Usually, in AR-coating design the index of refraction of the films is not a variable parameter. More layers are thus needed to obtain proper admittance matching with the available indices of refraction. In the $Al_xGa_{1-x}As$ native-oxide material system, the index of refraction of the oxide layer is also not widely variable. However, the index of the semiconductor can be continuously varied between ~2.9 (AlAs) and ~3.5 (GaAs). Having this available toolbox of indices greatly increases the flexibility of the coating design. A lower reflectance value can be achieved by using a second semiconductor layer of variable index to match between the oxide layer and the substrate. A second layer also broadens the low reflectance region. The design of a two-layer AR coating in which the optical thickness of the oxide and matching layers are fixed at a quarter wavelength and the index is calculated to exactly match admittances is straightforward.[6] Fixing the thickness and calculating the index assures reasonably thick layers and has historically aided in optical monitoring during deposition. The calculation of the needed index involves equating the admittance of the incident medium with the equivalent admittance of the coating. The result is

$$n_0 = \frac{n_1^2 n_3}{n_2}. \tag{2}$$

The variables of Eq. (2) are defined in the vector diagram shown in Fig. 3, where n_2 now represents the index of the second film layer and n_3 represents the index of the substrate. The phase thicknesses of the two film layers are denoted by δ_1 and δ_2. The three material interfaces are labeled *a*, *b*, and *c*.

Solving for n_2 using the indices of electron-beam-deposited Al_2O_3,GaAs (at 1 μm), and air yields a value of 3.29. This corresponds to an $Al_xGa_{1-x}As$ layer with an Al composition of 39%. However, for an assumed oxide index of 1.57, the needed matching index (n_2) is 2.92, very near the lowest achievable index in the $Al_xGa_{1-x}As$ material system. Additionally, the higher the aluminum composition, the harder it will be to accurately control the thickness of the surface oxide layer as the oxidation selectivity is reduced.[8] Figure 4 illustrates the needed matching layer index and equivalent composition for a given surface layer index. Alternatively, a device may require matching between air and an equivalent index less than that of GaAs. The index of the oxide layer and the available range of $Al_xGa_{1-x}As$ indices limit the range of substrate compositions which can be exactly matched. Parallel lines to the left of the solid line of Fig. 4 can be drawn to represent lower equivalent substrate indices. The x intercept is the square root of the substrate index. A quarter–quarter AR coating of ($n_1 = 1.57$)/AlAs on

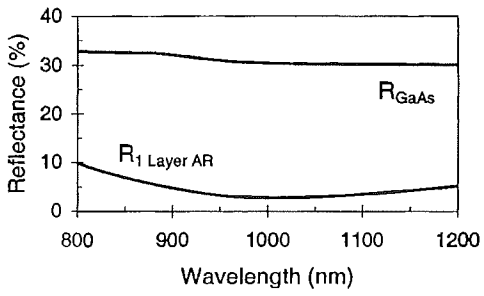

FIG. 2. The theoretical reflectance from a one-layer quarter-wave coating with $n_1 = 1.57$ (all wavelengths) on a GaAs substrate. The reflectance of uncoated GaAs is also shown.

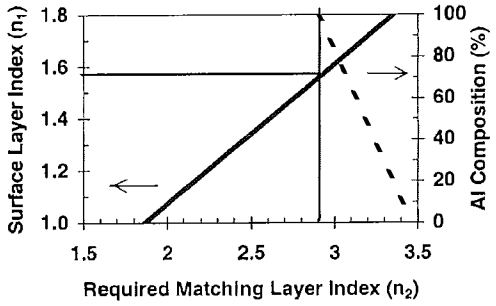

FIG. 4. Plot of the necessary matching layer index and equivalent composition for a given surface layer index to achieve zero reflectance at 1 μm with a quarter–quarter coating on GaAs.

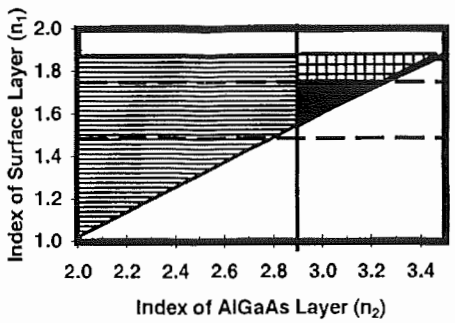

FIG. 5. A modified Schuster diagram for a two-layer AR coating. The solid black filled region represents the region of zero reflectance solutions given the constraints of the oxide index, available AlGaAs indexes for an incident medium of air and a GaAs substrate (at 1 μm).

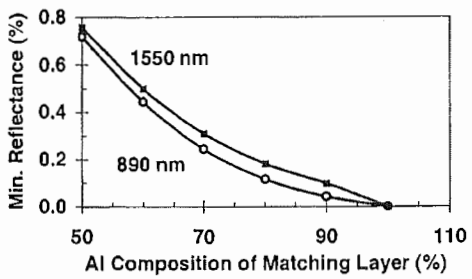

FIG. 6. Plot of the calculated reflectance minimum for a quarter–quarter coating vs aluminum composition of the matching layer for design wavelengths of 890 and 1550 nm. An oxide index of 1.57, a substrate of GaAs and an incident medium of air are used.

GaAs has a calculated reflectance minimum of 1.6×10^{-3} % and exhibits a reflectance of <1% over a 400 nm range about its design wavelength of 1 μm.

C. Two-layer antireflection coating (arbitrary thickness)

1. Surface oxide

A problem with the two-layer coating above is the limited range of substrate indices that can be matched for a given oxide index because of the available $Al_xGa_{1-x}As$ index values. Additionally, the necessarily high Al composition of the matching layer makes manufacturing more difficult. For a coating that is not forced to be constructed of layers a quarter wavelength thick, the layer materials can be chosen from a range of indices and the coating thickness adjusted to suit. This allows flexibility in choosing oxidation selectivity and layer thicknesses.

A set of equations for the phase thicknesses of the two layers can be obtained by writing out the characteristic matrix for the assembly and equating the real and imaginary parts of the layers' admittance, separately, to the admittance of the incident medium.[6] The equations for the phase thickness of the two layers are

$$\tan^2 \delta_1 = \frac{(n_3 - n_0)(n_2^2 - n_0 n_3) n_1^2}{(r_1^2 n_3 - n_0 n_2^2)(n_0 n_3 - r_1^2)}, \tag{3}$$

$$\tan \delta_1 \tan \delta_2 = \frac{n_1 n_2 (n_3 - n_0)}{n_1^2 n_3 - n_0 n_2^2}. \tag{4}$$

The phase thickness is then related to the physical thickness by

$$\delta = \frac{2\pi n d}{\lambda}, \tag{5}$$

where n is the index of the layer, d is its physical thickness, λ is the wavelength of the design, and normal incidence has been assumed.

A Schuster diagram is a useful way to represent pairs of real solutions to Eqs. (3) and (4).[6,9] A modified form of the Schuster diagram is shown in Fig. 5. Again taking n_0 as air, n_1 as oxide, n_2 as $Al_xGa_{1-x}As$, and n_3 as the GaAs substrate, the region satisfying the equations for zero reflectance are filled with a light hashing. Dotted horizontal lines at $n_1 = 1.5$ and 1.75 bound the range of indices between wet-oxidized AlGaAs and electron-beam-deposited Al_2O_3. A vertical line indicating the lowest achievable $Al_xGa_{1-x}As$ index (~2.9) for layer two is also shown. The triangular dark checkered region represents the real solutions for n_2 indices achievable in the $Al_xGa_{1-x}As$ material system. The solid black fill shows the subset region obtained by logically ANDing the constraints of the oxide index, available $Al_xGa_{1-x}As$ indexes, and the region satisfying the mathematics for zero reflectance for an incident medium of air and a GaAs substrate. While this coating scheme yields a range of possible indices for n_2 for a given n_1 index, the overall region is limited. For an oxide index of 1.57, a real solution is achievable only with an AlAs matching layer. Additionally, this solid black filled region shrinks as the substrate index is lowered.

The Schuster diagram displays solutions that yield zero reflectance. It provides little information regarding solutions with minimum reflectance when a zero reflectance solution does not exist. To aid in the coating's manufacture, we generally want to use a lower Al composition and thus higher n_2. This is the region in Fig. 5 to the right of the diagonal line. By minimizing the equations for the reflectance of the assembly, we find that the lowest reflectance in this situation is achieved for quarter–quarter coatings. Quarter–quarter coatings, represented by Eq. (2), are illustrated on the Schuster diagram by the diagonal line. Figure 6 shows the calculated reflectance minimum for a quarter–quarter coating versus Al composition of the matching layer for 890 and 1550 nm. Figure 6 uses an oxide index of 1.57, a substrate of GaAs, and an incident medium of air. Despite the nonexistence of a zero solution, reflectance minima of a few tenths of one percent can be achieved for matching layers with aluminum compositions as low as 70%.

2. Buried oxide

In (1), the topmost layer of the coating was oxide. By expanding the axis range of the Schuster diagram, real solutions exist when n_1 is greater than n_2. Thus, by switching to a buried oxide layer rather than a surface oxide layer, the region of real solutions is substantially increased. Figure 7 illustrates this. Two dotted vertical lines at $n_2 = 1.5$ and 1.75 bound the range of indices between wet-oxidized AlGaAs

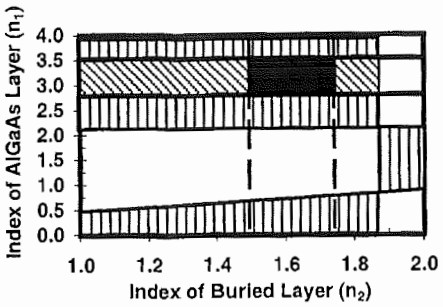

FIG. 7. A modified Schuster diagram for a buried-oxide Ar coating. The rectangular solid black filled region indicates that an AR coating can be designed for zero reflectance using wet-oxidized AlGaAs and a matching layer of any Al composition for any substrate with an effective index between 2.5 and 3.5.

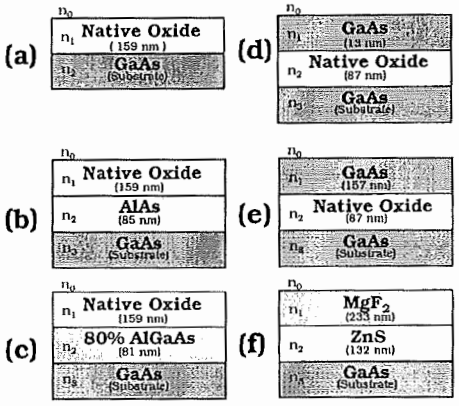

FIG. 8. Summary of five native-oxide AR coatings designed and simulated. The sixth coating, *F*, is a typical AR coating of ZnS/MgF_2 simulated for comparison.

and electron-beam-deposited Al_2O_3 for reference. The solid black filled region is now a rectangle rather than a triangle. This rectangle indicates that an AR coating can be designed for zero reflectance using a matching layer of any Al composition and a buried layer with any index from near wet thermally oxidized AlGaAs to even higher than that for electron beam deposited Al_2O_3. The thicknesses of the coating layers are adjusted to match admittances. Additionally, any effective substrate index between 2.5 and 3.5 can be properly matched with a buried layer of native oxide and an $Al_xGa_{1-x}As$ matching layer of any Al composition.

Further, the thickness of the cap layer can be increased independently of the oxide thickness by shifting the tangent solution by π [see Eqs. (3) and (4)]. This allows the capping layer thickness to be increased from tens to hundreds of nanometers at the expense of reduced bandwidth. We have had difficulty fabricating thin capping layer designs using a planar laterally oxidized structure[10] over large hole spacings ($\sim$150 μm). The long oxidation time required (1–2 h) causes significant surface oxidation and delamination of the cap layer.

The two-layer buried geometry provides the most flexibility in the coating's design. Tradeoffs in thickness and Al composition can easily be made for a given oxide index, effective substrate index, and design wavelength.

D. Native oxide AR coating performance

We have designed and simulated five different coatings to serve as examples of the performance anticipated from native-oxide AR coatings. We have also simulated a typical AR coating of ZnS/MgF_2 for comparison. Due to the broad spectral bandwidth of these coatings (hundreds of nanometers), careful consideration of the dispersion in the semiconductor and native oxide is important. We have used Terry's nine-harmonic oscillator model[11] for the index of all compositions of $Al_xGa_{1-x}As$ with the exception of AlAs, where we have used the Afromovitz model.[12] Previously,[13] we have reported the index of refraction of surface native-oxide layers analyzed by variable-angle spectroscopic ellipsometry over the wavelength range of 240–1700 nm. This data was fit with a Cauchy dispersion formula and used for the simulations of this section. The dispersion formula and parameters used are given by

$$n(\lambda)=1.5713+\frac{4.83\times10^{-3}}{\lambda^2}+\frac{9.67\times10^{-5}}{\lambda^4}, \tag{6}$$

where λ is in micrometers. These accurate index measurements allowed us to obtain excellent performance of our coatings using initial designs. Thickness of the coating layer was not changed from the predictions of our model. The center wavelength of the five coating designs is 1 μm. The characteristic matrix method was used for the calculation of the reflectance spectra.[14]

Coating *A* is simply a quarter-wave thick (159 nm) layer of native oxide on a substrate of GaAs. Coating *B* is a quarter wavelength of surface oxide on a quarter-wave thick AlAs layer (85 nm) on top of a GaAs substrate. Coating *C* is a quarter–quarter, surface-oxide coating of native oxide on $Al_{0.8}Ga_{0.20}As$ (81 nm) on top of a substrate of GaAs. Coating *D* an 87 nm thick, buried oxide layer, sandwiched between a GaAs substrate and a 13 nm capping layer of GaAs. Coating *E* is an 87 nm thick, buried oxide layer, sandwiched between a GaAs substrate and a 157 nm thick, "π-shifted," capping layer of GaAs. Coating *F* is a layer of MgF_2 ($n=1.38$,233 nm) on ZnS($n=2.3$,132 nm) on top a substrate of GaAs. These six coatings are summarized in Fig. 8.

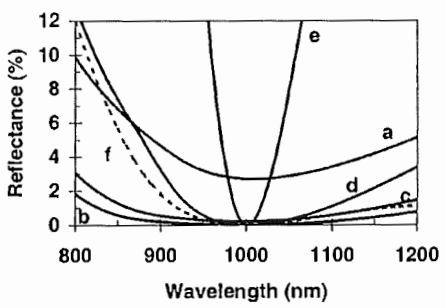

FIG. 9. The calculated reflectance of the six coatings summarized in Fig. 8.

The calculated reflectance spectrum of each coating is shown in Fig. 9. As discussed in Sec. II.A, the achievable reflectance minimum of coating A is fundamentally limited to several percent due to the admittance mismatch. The two-layer surface-oxide coating, B, exhibits a very near theoretical zero solution of $1.6\times 10^{-3}\%$. Coating B has a reflectance of less than 1% over 400 nm. If the center wavelength of the design is shifted further past the absorption edge of the GaAs substrate to 1300 nm, this range is extended to slightly over 500 nm. Coating C consists of a surface oxide with a matching layer that does not provide a zero reflectance solution. The calculated minimum reflectance of this coating is 0.21%. The reflectance is less than 1% over 290 nm. Coatings D and E are buried oxide coatings. While both have a theoretical minimum reflectance of 0, the region of low reflectance for buried coatings is significantly less than surface oxide coatings. Coating D has a reflectance of less than 1% over 158 nm. The π-shifted cap of coating E further reduces this region to 30 nm.

Excellent broad-bandwidth response is achieved for both surface and buried geometries. Comparing their performance to coating F, a conventional ZnS/MgF_2 coating (dashed line in Fig. 9), shows that surface-oxide AR coatings offer broader bandwidths with slightly higher reflectance minima. Buried oxides provide zero-reflectance solutions with a narrower spectral bandwidth. Choice of the coating geometry primarily depends on the device design (aperture size and effective substrate index).

III. FABRICATION

A conventional antireflection coating used on semiconductor devices is ZnS/MgF_2. Such a coating is typically deposited by evaporation. Before deposition, the sample must be scrupulously cleaned to remove any small particles present on the wafer. This cleaning step is very important since pinholes in the deposited film are easily formed. The complete evaporation setup consists of a vacuum chamber, cryogenic pumps, power supplies for the crucible heaters, thickness monitoring equipment, and a substrate heater. Additionally, process gases are needed to control the film's stoichiometry.

In this work, antireflection coatings are fabricated using buried or surface layer native-oxide films produced by wet thermal oxidation at atmospheric pressure of AlGaAs layers of high Al content. Since oxidation depends highly on Al composition, no thickness monitoring equipment is needed.[8] The simplicity of wet thermal oxidation significantly reduces the manufacturing complexities associated with conventional AR coating deposition on semiconductor devices.

All samples were grown by molecular beam epitaxy at a substrate temperature of 580 °C. The layers to be oxidized were $Al_{0.98}Ga_{0.02}As$, grown as a digital alloy with a 6 nm (5.5 nm AlAs,0.5 nm $Al_{0.50}Ga_{0.50}As$) period. All oxidations were carried out at 450 °C in a three-zone tube furnace under a 1 L/min flow of nitrogen gas bubbled through deionized water heated to 75 °C. A solvent cleaning was performed immediately before loading each sample into the furnace. A root-mean-square (rms) roughness of 0.5 nm for the surface oxides was measured by atomic force microscopy (AFM).[13] Pinholes in the coatings were not observed.

The surface oxide growths were either terminated on the high Al containing layer or capped with a sacrificial 10 nm layer of GaAs. Uncapped samples were oxidized immediately upon removal from the ultrahigh vacuum of the reactor to limit atmospheric hydrolization. For the capped samples, an etching solution of citric acid (50% by mass) and hydrogen peroxide (30%) (10:1 by volume) was used to remove the cap layer immediately before wet oxidation. The oxidation time for the surface oxide samples was several minutes.

The buried oxide epitaxial material was etched down to the substrate in 50 μm diameter pillars using a 1:6:40 solution of H_2SO_4:H_2O_2:H_2O. An optical microscope was used to determine the position of the oxide front. We observed a linear oxidation rate of $\sim$1 μm/min. The buried coating samples were oxidized 24 min.

The surface and buried geometries inherently lend themselves to different device applications. The surface geometry is useful for devices with optical apertures anywhere from a few micrometers to a full wafer. This is because the reaction front progresses longitudinally through the thin $Al_{0.98}Ga_{0.02}As$ layer. The reaction front does not need to travel transversely across the optical aperture as in the case of the buried geometry. The buried geometry is therefore limited to device apertures smaller than $\sim$100 μm. Native-oxide AR coatings can be integrated with current-confining oxide apertures in both geometries. Since the surface oxidation will progress significantly faster than the transverse oxidation needed to form the aperture, the formation of a surface AR coating does not impose limits on the aperture size. In the buried geometry, oxidation selectivity can be used to allow the AR coating to fully close across the optical aperture as the current aperture arrives at the correct diameter.

IV. EXPERIMENT

A. Surface-oxide AR coatings

1. Single layer coating

To demonstrate the simplest native-oxide AR coating, a single layer of $Al_{0.98}Ga_{0.02}As$ was grown, and a quarter-wafer sample was oxidized for 12 min. A 164 nm thick layer of oxide was produced on top of a GaAs substrate. Variable angle spectroscopic ellipsometry was used to determine the index of refraction and physical thickness. A layer contraction of $<$2% was determined by comparing reflectance fits of the unoxidized sample with the measured oxide thickness. Ellipsometry indicated an abrupt interface between the oxide and substrate and a small surface roughness as confirmed with AFM.[13] The reflectance of this sample (and all surface oxide samples) was measured with a spectrophotometer from 0.6 to 2 μm having an uncertainty of 0.05%. The measured reflectance was calibrated to a National Institute of Standards and Technology traceable standard with a stated uncertainty of 0.005%. The sample's reflectance is shown in Fig. 10. The sample has a minimum reflectance of $\sim$2.9% and a reflectance of less than 5% over 330 nm. We observed excellent

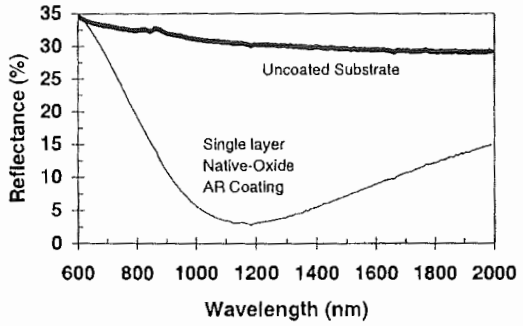

FIG. 10. The measured reflectance of a single-layer native-oxide AR coating. The measured reflectance of an uncoated substrate of GaAs is also shown.

thickness uniformity across the entire quarter wafer. The measured reflectance of an uncoated GaAs substrate is also shown in Fig. 10 for comparison.

2. Two layer coating

To lower and broaden the reflectance minimum we have fabricated two layer surface-oxide coatings. We have designed a coating with a matching layer of $Al_{0.80}Ga_{0.20}As$ to yield an oxidation selectivity of 100:1[8] at the expense of increasing the minimum reflectance. The design is coating *C* shown in Fig. 8. A quarter-wafer sample was placed in the furnace for 6 min. Simultaneously, the reflectance of another quarter-wafer sample was also measured for the oxidized sample. The reflectance spectrum of the as-grown and oxidized samples are shown in Fig. 11. A reflectance minimum of $0.41\pm0.06\%$ at 1 μm was measured by fitting a third-order polynomial around the minimum ($\sim\pm125$ nm) and calculating the standard deviation of the fit. The reflectance of the sample is less than 1% over >250 nm. The calculated minimum reflectance for the design as discussed in Sec. II.D is 0.21%. Variable angle spectroscopic ellipsometry of the fabricated coating has determined that the oxide thickness is 176 nm and the $Al_{0.80}Ga_{0.20}As$ matching layer is 74 nm thick. A reduction in the index by ~0.04 (at 1 μm) from that given in Eq. (6) was also determined. Calculation of the coating's minimum reflectance with these adjusted parameters yields a reflectance minimum of 0.36%, which is close to the measured minimum.

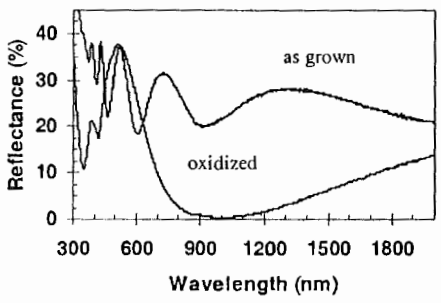

FIG. 11. The measured reflectance of the as-grown and oxidized samples of the oxide/$Al_{0.80}Ga_{0.20}As$ two-layer coating.

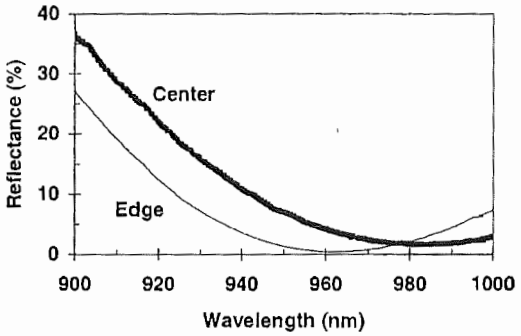

FIG. 12. The measured reflectance for the center and edge regions of a buried oxide coating on a 50 μm pillar. The center exhibits a higher minimum of reflectance as it is not fully oxidized, that is, the oxide aperture has not fully closed in across the pillar.

Optical scattering loss from the first surface can be calculated for the surface oxide samples using the rms roughness from the AFM data (0.5 nm), assuming a Gaussian distribution of heights and normally incident illumination with a wavelength of 1 μm.[15] The calculated optical scattering loss per pass is $2.1\times10^{-4}\%$. This scattering loss indicates the order of magnitude of the anticipated transmittance ultimately achievable through surface oxide AR coatings.

B. Buried oxide AR coating

We have fabricated coating *E* shown in Fig. 8. Coating *E* is a π-shifted design. Compositional grading was used over 20 nm at the GaAs–$Al_{0.98}Ga_{0.02}As$ interfaces to avoid delamination after oxidation.[4]

In order to measure the reflectance of the etched 50 μm pillars, a Ti:sapphire laser beam was focused using a microscope objective to a ~2 μm diameter spot with an incident half-angle cone of $\sim25°$ and scanned in wavelength from 900 to 1000 nm. An InGaAs detector collected the reflected light and the higher intensity transmitted light was trapped by a beam dump. Irises were used to block the scattered light from the unpolished back of the substrate. The measured sample's reflectance was calibrated to the front surface reflection off a fused-quartz optical flat.[16] Care was taken to ensure that the sample and flat were measured in the same focal plane. Lock-in detection at 2 kHz was used to obtain a high signal–noise ratio. A measurement uncertainty of 0.2% is estimated.

Gradations in oxide thickness due to incomplete oxidation were seen by imaging the sample pillars with the monochromatic laser light and observing the contrast of the image. When the laser was tuned to near the designed wavelength of minimum reflectance, the outermost regions of the pillar appeared as a dark ring while the center and substrate appeared brighter.

Figure 12 shows the measured reflectance for the center and edge regions of the pillar. The fully oxidized edge has a minimum reflectance at 960 nm of 0.4% and a reflectance of <1% over 21 nm. The minimum reflectance of the partially oxidized center region has shifted to near 980 nm and has increased to 1.6%. The nonzero minimum of reflectance measured at the edge is attributed to the semiconductor lay-

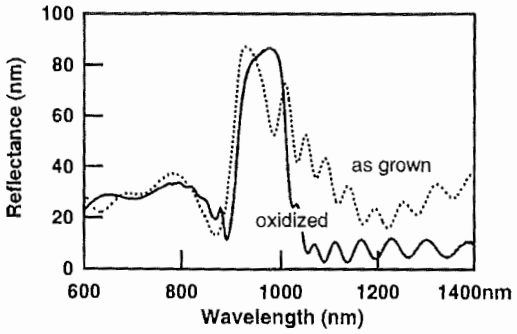

FIG. 13. The measured reflectance of a semiconductor saturable absorber mirror with a two-layer native-oxide AR coating before and after 5 min of oxidation. The Fabry–Perot resonance is eliminated after oxidation.

ers being thinner than designed. A small index variation, as discussed in Sec. II.A.2, can also lead to a few tenths of one percent increase in the minimum reflectance.

C. Integration with a saturable absorbing mirror

Intracavity semiconductor saturable absorber mirrors (SESAMs) are important for compact mode-locked or Q-switched solid-state laser systems. We have integrated a native-oxide AR coating with an antiresonant Fabry–Perot SESAM[17] to demonstrate application to a multilayer device. An AR coating is required on this device to avoid Fabry–Perot resonance effects and increase the intensity entering the semiconductor saturable absorber to reduce the effective saturation intensity. The AR coating must be broadband and have minimal group velocity dispersion. Al_2O_3 is typically used for these needs.[17] Native-oxide AR coatings also satisfy these requirements.

The antiresonant SESAM design for 1020 nm consists of nine $In_{0.25}Ga_{0.75}As$ quantum wells with GaAs barriers on top of a 20-pair AlAs/GaAs bottom DBR. An equivalent index for the structure was determined by first calculating the optical penetration distance into the bottom DBR and adding the optical path length of the rest of the structure assuming a constant field intensity. Dividing by the sum of the effective bottom mirror thickness and the physical thickness of the rest of the structure, yields an effective index of 3.34.

A surface-oxide coating was designed to minimize the reflectance from this effective substrate using a matching layer of $Al_{0.80}Ga_{0.20}As$. A zero reflectance solution does not exist for this coating; a minimum of 0.45% was calculated for a quarter–quarter coating. Figure 13 shows the reflectance spectrum of the SESAM before (dashed line) and after 5 min of oxidation (solid line). The Fabry–Perot resonance at 980 nm present in the as-grown spectrum, due to the reflection from the semiconductor–air interface, disappears after oxidation.

V. SUMMARY AND CONCLUSION

In summary, we have developed two-layer native-oxide antireflection coatings in two geometries: buried and surface. We have studied and reported the design criteria surrounding each of these two geometries. We have mathematically shown that surface oxide coatings can offer a nearly zero minimum of reflectance and a reflectance of $<1\%$ over 500 nm for the case of an AlAs matching layer. Reducing the Al composition in the AlGaAs matching layer to 80% yields a coating with a reflectance minimum of 0.2% and a reflectance of $<1\%$ over nearly 300 nm. Buried oxide coatings can be designed to exactly match the admittance of any substrate with effective index between 2.5 and 3.5 using a matching layer of any Al composition and a buried layer with any index near that of wet thermally oxidized $Al_xGa_{1-x}As$. Buried coatings with a zero reflectance minimum and a $<1\%$ reflectance bandwidth of >150 nm have been designed and simulated.

We have experimentally demonstrated a surface coating having a reflectance minimum of 0.4% and a reflectance of $<1\%$ over >250 nm. We have additionally developed a π-shifted buried-oxide coating having a reflectance minimum of 0.4% and a reflectance of $<1\%$ over 21 nm. We have also shown integration of a native-oxide AR coating with the multilayer structure of a semiconductor saturable absorber mirror in order to remove the Fabry–Perot resonance and thus reduce the effective saturation intensity. The calculated optical scattering loss from measured roughness data indicates that reflectance minima as low as $10^{-4}\%$ are ultimately achievable with native-oxide antireflection coatings.

Native-oxide AR coatings reduce manufacturing complexity and cost while promoting integration with other developing native-oxide technologies and rivaling the performance of traditionally deposited coatings.

This work is a contribution of the United States government by the National Institute of Standards and Technology (NIST) and is not subject to copyright.

[1] J. M. Dallesasse, N. Holonyak, Jr., A. R. Sugg, T. A. Richard, and El-Zein, Appl. Phys. Lett. **57**, 2844 (1990).
[2] J. M. Dallesasse and N. Holonyak, Jr., Appl. Phys. Lett. **58**, 394 (1991).
[3] D. L. Huffaker, D. G. Deppe, K. Kumar, and T. J. Rogers, Appl. Phys. Lett. **65**, 97 (1994).
[4] M. H. MacDougal, P. D. Dapkus, A. E. Bond, C. K. Lin, and J. Geske, IEEE J. Sel. Top. Quantum Electron. **3**, 905 (1997).
[5] W. A. Loong and H. L. Chaung, Jpn. J. Appl. Phys., Part 2 **30**, L1319 (1991).
[6] H. A. Macleod, *Thin-Film Optical Filters* (American Elsevier, New York, 1969).
[7] A. K. Chin, G. Zydzik, S. Singh, L. G. Van Uitert, and G. Minneci, J. Vac. Sci. Technol. B **1**, 72 (1983).
[8] K. D. Choquette *et al.* IEEE J. Sel. Top. Quantum Electron. **3**, 916 (1997).
[9] K. Schuster, Ann. Phys. (Leipzig) **4**, 352 (1949).
[10] C. L. Chua, R. L. Thorton, and D. W. Treat, IEEE Photonics Technol. Lett. **9**, 1060 (1997).
[11] F. L. Terry, Jr., J. Appl. Phys. **70**, 409 (1991).
[12] M. A. Afromovitz, Solid State Commun. **15**, 59 (1974).
[13] K. J. Knopp, R. P. Mirin, D. H. Christensen, K. A. Bertnesss, A. Roshko, and R. A. Synowicki, Appl. Phys. Lett. **73**, 3512 (1998).
[14] M. Born and E. Wolf, *Principles of Optics*, 6th ed. (Pergamon, New York, 1980).
[15] H. E. Bennett and J. O. Porteus, J. Opt. Soc. Am. **51**, 123 (1961).
[16] W. S. Rodney and R. J. Spindler, J. Res. Natl. Bur. Stand. **53**, 185 (1954).
[17] U. Keller *et al.*, IEEE J. Sel. Top. Quantum Electron. **2**, 435 (1996).